

Compact Tri-Band Meandered Ring Monopole Antenna with Two Embedded Strips for WLAN/WiMAX Applications

Hong Chen^{*}, Ying-Zeng Yin, and Jian-Jun Wu

Abstract—A novel coplanar waveguide (CPW)-fed tri-band monopole antenna for WLAN/WiMAX applications is presented. To get a compact antenna size, meandering and coupling technologies are used here. Meanwhile, with the loading method, the higher mode is used to cover the required band. The antenna has a very small size of only $18 \times 28 \text{ mm}^2$. The measured and simulated results show that the proposed antenna has three separate 10-dB impedance bandwidths of 220 MHz (2.36–2.58 GHz), 470 MHz (3.36–3.83 GHz) and 1460 MHz (4.83–6.29 GHz), which can cover all the 2.4/5.2/5.8 GHz WLAN and 3.5/5.5 GHz WiMAX bands. Good dipole-like radiation characteristics are obtained over the operating bands.

1. INTRODUCTION

Nowadays, the Wireless Local Area Network (WLAN) and Worldwide Interoperability for Microwave Access (WiMAX) are popular networks for accessing the internet. In order to support the WLAN/WiMAX applications, multiband antennas with high performance, compact size and simple structure are required. Planar monopole antennas are very suitable for WLAN/WiMAX applications due to their advantageous features, such as low profile, light weight, and easy fabrications. However, due to the required length of monopole antenna for resonating in the lower band, the antenna size is relatively large. The usual technology for size reduction is meandering. The strips responsible for the lower band are meandered into different shapes, such as triangle shape [1], U-shape [2,3], and ring shape [4–6]. Introducing the coupling between different strips responsible for the different bands is another technology for size reduction [3,7]. The coupling can produce capacitance, which shift the resonant frequencies toward lower frequencies.

In this paper, the meandering and coupling technologies are used to design a compact tri-band monopole antenna. Meanwhile, to make the higher mode of the meandered ring shift down to cover the 5.2/5.5 GHz WLAN and 5.5 GHz WiMAX band, the loading technology [8,9] is used here. The proposed antenna consists of a meandered ring, an embedded inverted T-shaped strip, and an embedded T-shaped strip. The total size of the proposed antenna is only $18 \times 28 \text{ mm}^2$, which is smaller than the antennas for WLAN/WiMAX applications [1–6,10,11]. Furthermore, as demonstrated in the next sections, the proposed antenna has three distinct bands, which can cover all the 2.4/5.2/5.8 GHz WLAN and 3.5/5.5 GHz WiMAX bands. Details of design considerations and the simulated and measured results are presented in the next sections.

2. ANTENNA DESIGN CONSIDERATIONS

The design evolution process for the proposed antenna is shown in Figure 1. The antenna is designed and optimized by using the ANSYS HFSS 13. The various antennas involved in Figure 1 are designed

Received 24 February 2014, Accepted 25 March 2014, Scheduled 27 March 2014

^{*} Corresponding author: Hong Chen (keyan_ch2013@163.com).

The authors are with the National Laboratory of Science and Technology on Antennas and Microwaves, Xidian University, Xi'an, Shaanxi 710071, P. R. China.

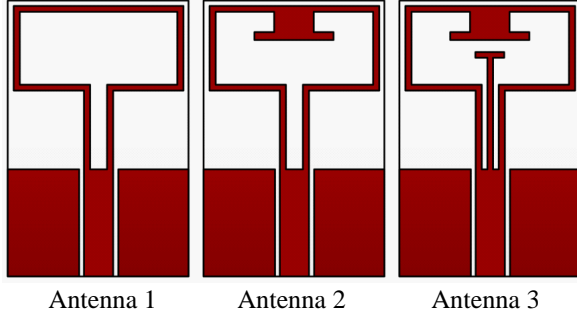


Figure 1. The design evolution process of the proposed antenna.

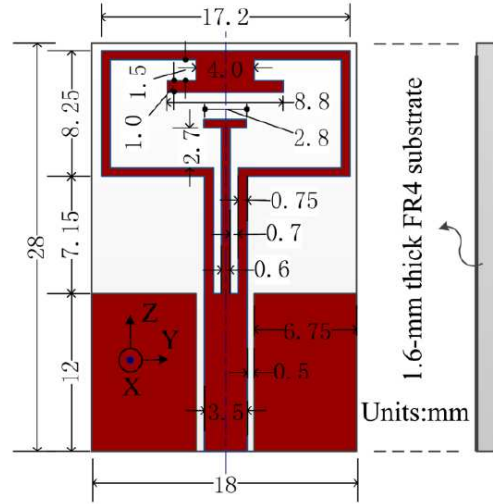


Figure 2. The configuration of the proposed antenna.

on a 1.6-mm thick FR4 substrate with relative permittivity of 4.4 and loss tangent of 0.02. A 50- Ω CPW transmission line with signal strip width of 3.5 mm and a gap distance of 0.5 mm between the signal strip and the ground plane is used for feeding the antenna.

Antenna 1 in Figure 1 is designed to excite a resonant mode covering the 2.4 WLAN band, and is formed by properly meandering the two straight trips of a monopole antenna resonating at about 2.4 GHz into a meandered ring. In order to get a compact antenna size for design, an inverted T-shaped strip is embedded in the meandered ring (see Antenna 2 in Figure 1). The loading inverted T-shaped strip is used to shift the higher mode toward lower frequencies to cover the 5.2/5.5 GHz WLAN and 5.5 WiMAX bands and improve the impedance matching. Detailed effects of the loading inverted T-shaped strip on the antenna performance will be discussed in Figure 5 in the next section.

A T-shaped strip is embedded in the meandered ring of Antenna 2 to excite a mode at 3.5 GHz to cover the 3.5 GHz WiMAX band. Thus, the Antenna 3 in Figure 1 is formed. The two embedded strips are T-shaped largely because this shape is helpful in achieving a compact antenna size. Note that, because the proposed antenna can introduce the electromagnetic coupling between the meandered ring and the T-shaped strip, which could lower the resonant frequencies, the antenna size would be further reduced.

The design mechanism will be further discussed and validated in the next section. Based on the configuration of Antenna 3, a final design can be obtained by further optimizing the dimensions. The optimized dimensions of the proposed antenna are clearly given in Figure 2.

3. RESULTS AND DISCUSSION

Based on the dimensions given in Figure 2, a prototype for the proposed antenna is fabricated and measured. A photograph of the prototype is exhibited in Figure 3. The return losses of the prototype were measured using the Agilent E8363B vector network analyzer. The simulated and measured return losses are shown in Figure 3. Good agreement between measured data and simulated results is obtained. The three 10-dB measured impedance bandwidths for the lower, middle and upper bands, respectively, reach 220 MHz (2.36–2.58 GHz), 470 MHz (3.36–3.83 GHz) and 1460 MHz (4.83–6.29 GHz), which can cover all the 2.4 (2.4–2.484 GHz)/5.2 (5.15–5.35 GHz)/5.8 (5.725–5.825 GHz) WLAN and 3.5 (3.4–3.69 GHz)/5.5 (5.25–5.85 GHz) WiMAX bands.

To investigate the radiation mechanism, the simulated surface current distributions of the proposed antenna at 2.4, 3.5 and 5.5 GHz are shown in Figure 4. Results in Figure 4(a) show that at 2.5 GHz the surface currents distribute mainly along the external meandered ring, which demonstrates that the meandered ring is the major radiating element for the lower band. Note that the surface current

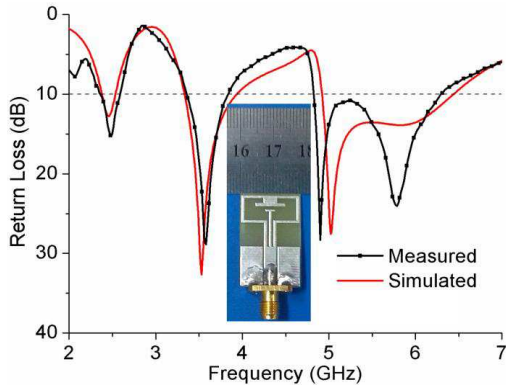


Figure 3. Simulated and measured return losses of the proposed antenna.

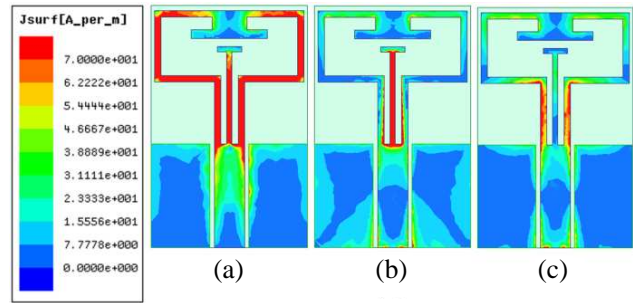


Figure 4. Simulated surface current distributions of the proposed antenna at (a) 2.4, (b) 3.5, and (c) 5.5 GHz.

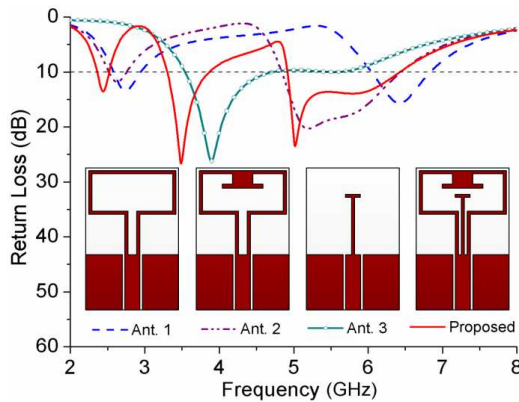


Figure 5. Simulated return losses of the various antenna structures involved.

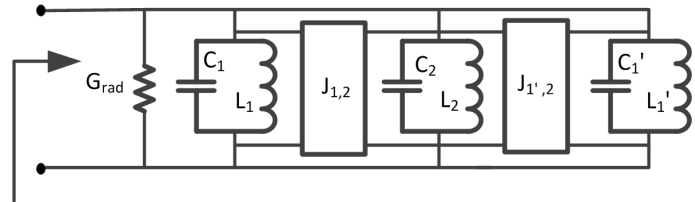


Figure 6. Equivalent circuit model of the proposed antenna.

distribution on the T-shaped strip is large due to the electromagnetic coupling between the T-shaped strip and meandered ring. At 3.5 GHz, most of surface currents flow along the T-shaped strip as shown in Figure 4(b), which indicates that the internal T-shaped strip contributes to the resonance for the middle band. Figure 4(c) shows that at 5.5 GHz larger surface currents concentrate on the meandered ring and one current null can be found along the meandered ring, which demonstrates that the proposed antenna operates as higher mode for the upper band.

In order to validate the design mechanism presented in the previous section, the simulated return losses of antenna with the meandered ring only (denoted as Antenna 1), the meandered ring with inverted T-shaped strip only (denoted as Antenna 2), and T-shaped strip only (denoted as Antenna 3), respectively, and the proposed monopole antenna (denoted as Proposed), are shown in Figure 5. Note that, as shown in Figure 5, the meandered ring (Antenna 1) excites a mode at about 2.75 GHz. This is largely because the length of meandered ring is approximately equal to half-wavelength at about 2.75 GHz. It can be seen that by embedding an inverted T-shaped strip in the meandered ring of Antenna 1, the higher mode of Antenna 2 is shifted down to about 5.5 GHz with good impedance matching. These behaviors are expected as discussed in Section 2. Compared with Antenna 1, Antenna 2 and Antenna 3, the resonant frequencies in the lower and middle bands of the proposed antenna are obviously shifted toward lower frequencies. These demonstrate that the proposed antenna with smaller size is obtained by introducing the coupling between different radiating elements in the antenna design.

To understand clearly the mechanism of the proposed antenna, Figure 6 illustrates the equivalent circuit model. The meandered ring with inverted T-shaped strip (see Antenna 2 in Figure 5) is simply

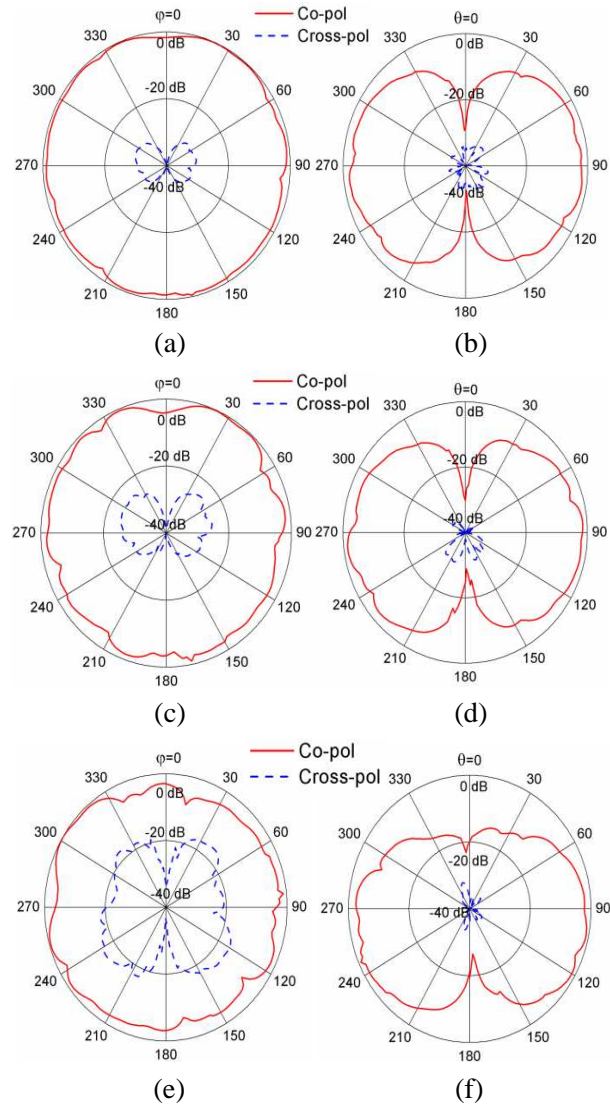


Figure 7. Measured radiation patterns for the proposed antenna at 2.4, 3.5 and 5.5 GHz. (a) *xy*-plane at 2.4 GHz. (b) *xoz*-plane at 2.4 GHz. (c) *xy*-plane at 3.5 GHz. (d) *xoz*-plane at 3.5 GHz. (e) *xy*-plane at 5.5 GHz. (f) *xoz*-plane at 5.5 GHz.

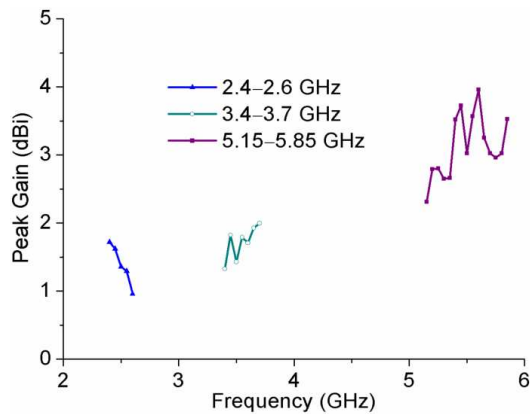


Figure 8. Measured antenna gains for the proposed antenna.

modeled by two lumped parallel resonant circuits (L_1, C_1) , (L'_1, C'_1) . Here, (L_1, C_1) and (L'_1, C'_1) represent Antenna 2 operates as first and second modes, respectively. The interior T-shaped (see Antenna 3 in Figure 5) can be simply modeled by a lumped parallel resonant circuit (L_2, C_2) . Two J-inverters (J, J') are used to describe the coupling between the interior T-shaped strip and the exterior meandered ring with inverted T-shaped strip. The G_{rad} represents the antenna radiation conductance. Obviously, due to the J-inverters, the resonant frequency of the equivalent circuit becomes smaller compared to the separate resonator (L_1, C_1) .

Radiation characteristics of the antenna prototype over the operating bands are measured. The radiation patterns and gains of the prototype were measured with SATIMO antenna measurement system in an anechoic chamber. The measured far-field normalized radiation patterns in xoy plane (H -plane) and xoz plane (E -plane) at 2.4, 3.5 and 5.5 GHz, respectively, are depicted in Figures 7(a)–(f). The dipole-like radiation patterns are observed. The measured peak gains for the antenna prototype are depicted in Figure 8. The measured peak gains in 2.4–2.6, 3.4–3.7 and 5.15–5.85 GHz bands, respectively, is 0.96–1.72 dBi, 1.33–2 dBi and 2.31–3.96 dBi.

4. CONCLUSION

A novel tri-band monopole antenna with very small size of only $18 \times 28 \text{ mm}^2$ is designed and implemented. Although the antenna has a compact size and simple structure, it can generate three broad bands to cover all the 2.4/5.2/5.8 GHz WLAN and 3.5/5.5 GHz WiMAX bands. Meanwhile, the antenna shows dipole-like radiation patterns over the operating bands. Due to its very compact size and good electromagnetic property, the proposed antenna could be a good candidate for practical WLAN/WiMAX applications.

REFERENCES

1. Chu, Q.-X. and L.-H. Ye, "Design of compact dual-wideband antenna with assemble monopoles," *IEEE Trans. Antennas Propag.*, Vol. 58, No. 12, 4063–4066, Dec. 2010.
2. Yoon, J.-H., "Fabrication and measurement of rectangular ring with open-ended CPW-fed monopole antenna for 2.4/5.2-GHz WLAN operation," *Microw. Opt. Technol. Lett.*, Vol. 48, No. 8, 1480–1483, Aug. 2006.
3. Koo, T.-W., D. Kim, J.-I. Ryu, J.-C. Kim, and J.-G. Yook, "A coupled dual-U-shaped monopole antenna for WiMAX triple-band operation," *Microw. Opt. Technol. Lett.*, Vol. 53, No. 4, 1745–1748, Apr. 2011.
4. Zhang, L., Y.-C. Jiao, G. Zhao, Y. Song, and F.-S. Zhang, "Broadband dual-band CPW-fed closed rectangular ring monopole antenna with a vertical strip for WLAN/WiMAX operation," *Microw. Opt. Technol. Lett.*, Vol. 50, No. 7, 1929–1931, Jul. 2008.
5. Zhang, Q.-Y. and Q.-X. Chu, "Triple-band dual rectangular ring printed monopole antenna for WLAN/WiMAX applications," *Microw. Opt. Technol. Lett.*, Vol. 51, No. 12, 1066–1073, Dec. 2009.
6. Ren, X.-S., Y.-Z. Yin, S.-F. Zheng, S.-L. Zuo, and B.-W. Liu, "Triple-band rectangular ring monopole antenna for WLAN/WiMAX applications," *Microw. Opt. Technol. Lett.*, Vol. 53, No. 5, 974–978, 2011.
7. Shams, K. M. Z. and M. Ali, "Study and design of a capacitively coupled polymeric internal antenna," *IEEE Trans. Antennas Propag.*, Vol. 53, No. 3, 985–993, Mar. 2005.
8. Chi, Y.-W. and K.-L. Wong, "Compact multiband folded loop chip antenna for small-size mobile phone," *IEEE Trans. Antennas Propag.*, Vol. 56, No. 12, 3797–3803, 2008.
9. Wong, K.-L. and C.-H. Huang, "Printed loop antenna with a perpendicular feed for penta-band mobile phone application," *IEEE Trans. Antennas Propag.*, Vol. 56, No. 7, 2138–2141, 2008.
10. Zhai, H.-Q., Z.-H. Ma, Y. Han, and C.-H. Liang, "A compact printed antenna for triple-band WLAN/WiMAX applications," *IEEE Antennas and Wireless Propag. Lett.*, Vol. 12, 65–68, Jul. 2013.
11. Hua, M.-J., P. Wang, Y. Zheng, and S. L. Yuan, "Compact tri-band CPW-fed antenna for WLAN/WiMAX applications," *IET Electron. Lett.*, Vol. 49, No. 18, 1118–1119, Aug. 2013.